

MIT Open Access Articles

All-sky search for short gravitational-wave bursts in the first Advanced LIGO run

The MIT Faculty has made this article openly available. *Please share* how this access benefits you. Your story matters.

Citation: Abbott, B. P. et al. "All-Sky Search for Short Gravitational-Wave Bursts in the First Advanced LIGO Run." *Physical Review D* 95.4 (2017): n. pag. © 2017 American Physical Society

As Published: <http://dx.doi.org/10.1103/PhysRevD.95.042003>

Publisher: American Physical Society

Persistent URL: <http://hdl.handle.net/1721.1/107412>

Version: Final published version: final published article, as it appeared in a journal, conference proceedings, or other formally published context

Terms of Use: Article is made available in accordance with the publisher's policy and may be subject to US copyright law. Please refer to the publisher's site for terms of use.



All-sky search for short gravitational-wave bursts in the first Advanced LIGO run

B. P. Abbott *et al.**

(LIGO Scientific Collaboration and Virgo Collaboration)

(Received 11 November 2016; published 16 February 2017)

We present the results from an all-sky search for short-duration gravitational waves in the data of the first run of the Advanced LIGO detectors between September 2015 and January 2016. The search algorithms use minimal assumptions on the signal morphology, so they are sensitive to a wide range of sources emitting gravitational waves. The analyses target transient signals with duration ranging from milliseconds to seconds over the frequency band of 32 to 4096 Hz. The first observed gravitational-wave event, GW150914, has been detected with high confidence in this search; the other known gravitational-wave event, GW151226, falls below the search's sensitivity. Besides GW150914, all of the search results are consistent with the expected rate of accidental noise coincidences. Finally, we estimate rate-density limits for a broad range of non-binary-black-hole transient gravitational-wave sources as a function of their gravitational radiation emission energy and their characteristic frequency. These rate-density upper limits are stricter than those previously published by an order of magnitude.

DOI: [10.1103/PhysRevD.95.042003](https://doi.org/10.1103/PhysRevD.95.042003)

I. INTRODUCTION

The first observing period of the Advanced LIGO detectors [1,2] has been completed recently with the most sensitive gravitational-wave (GW) detectors ever built. The two LIGO observatories in Hanford, Washington, and Livingston, Louisiana, achieved a major milestone in gravitational-wave astronomy: the first direct detection of gravitational waves on September 14, 2015, referred to as GW150914 [3]. Advanced LIGO is the first of a new generation of instruments, including GEO 600 [4], Advanced Virgo [2], KAGRA [5], and LIGO-India [6].

This paper reports on a search for short-duration transient gravitational-wave events, commonly referred to as GW bursts, during the first observing run (O1) of the Advanced LIGO detectors, from September 2015 to January 2016. The first 16 days of coincident data have already been analyzed, resulting in a high-significance detection statement for the GW150914 event [7]. GW bursts can be generated by a wide variety of astrophysical sources, such as merging compact binary systems [8,9], core-collapse supernovae of massive stars [10], neutron stars collapsing to form black holes, pulsar glitches, and cosmic string cusps [11]. Some of these sources have dedicated targeted searches such as optically triggered core-collapse supernova [12] or Gamma-Ray Bursts triggered searches [13]. To search broadly for these phenomena, we employ searches with minimal assumptions regarding the expected waveform characteristics and the source direction. The search we report here is more sensitive than the previous burst searches [14] because of both the increased sensitivity of the Advanced detectors [15] and

improvements in the search algorithms in rejecting transient non-Gaussian noise artifacts (glitches) [16–19].

The described unmodeled all-sky search for GW bursts consists of three different algorithms. This paper shows the result of these algorithms and gives limits on the rate density of transient GW events. All of these algorithms have independently claimed high-significance detections of GW150914 [7]. The lower-mass GW event, GW151226 [20], and the LVT151012 candidate [21,22] were not detected by these searches.

The paper is organized as follows. In Sec. II, we give an overview of the O1 data set. In Sec. III, we give a brief overview of the three search algorithms. The sensitivity of the search is described in Sec. IV. Finally, Secs. V and VI discuss the search results and their implications.

II. OBSERVING RUN 1

Our data set extends over 130 calendar days from September 12, 2015, to January 19, 2016. This first observing period (called O1) of Advanced LIGO began after a series of major upgrades to both the Hanford and Livingston detectors [3].

In the most sensitive frequency band, 100–300 Hz, the O1 LIGO detectors are three to five times more sensitive than the initial LIGO detectors [15]. Future observing runs are expected to increase sensitivity by an additional factor of 3 [6].

As in the previous LIGO/Virgo searches [23–25], intervals of poor data quality are identified and excluded from the analysis. To monitor environmental disturbances and their influence on the detectors, each observatory is equipped with an array of sensors: seismometers, accelerometers, microphones, magnetometers, radio receivers,

*Full author list given at the end of the article.

weather sensors, ac-power line monitors, and a cosmic-ray detector. Hundreds of thousands of auxiliary channels within the instrument are also monitored. Characterization of the relationship of the strain data to this additional information allows many non-GW transients to be removed with high statistical confidence [7,26].

The live time in which the two detectors were individually locked is about 79 days for H1 and 67 days for L1. After data quality flags have been applied, the total analyzable time is about 75 days for H1 and 65 days for L1. The coincident live time between H1 and L1 is about 48 days. The 16 days of coincident data that have already been analyzed in Ref. [7] are a subset of this coincident O1 live time. Finally, the estimated calibration uncertainty (1σ) below 2 kHz is less than 10% in amplitude and 10 deg in phase [27]. The calibration uncertainty above 2 kHz is less certain, although the limited data obtained at these frequencies suggest upper bounds of 20% in amplitude and 10 deg in phase. These estimates will be further refined through future measurements and analyses [28].

III. SEARCHES

This search covers the most sensitive frequency band of the involved detectors, i.e. 32–4096 Hz, and it consists of the same three burst algorithms used to measure the significance of GW150914 [7]. They consist of two end-to-end algorithms, coherent Waveburst (cWB) [19,29] and omicron-LIB (oLIB) [18], and a followup algorithm applied to cWB events, BayesWave (BW) [30,31]. Using multiple search algorithms has two advantages: it can provide independent validation of results, and it can also improve the search sensitivity in regions of parameter space where a single algorithm outperforms the others.

The three algorithms ran over the 48 days of coincident data. However, due to internal segmentation,¹ the cWB and BW pipelines only actually analyzed 44 days of this coincident data. The oLIB analysis loss time is negligible and thus oLIB analyzed close to the full 48 days.

The three algorithms also ran in low-latency mode during O1. This mode approximates the analysis presented in this paper, but in real time so as to enable potential electromagnetic followup of gravitational-wave candidates. In this mode, both cWB and oLIB produced independent alerts of the GW150914 event, and the result was validated by a BW followup [32].

To characterize the statistical rate of transient noise glitches occurring simultaneously at the two LIGO sites by chance, this analysis uses the time-shift method: data from one interferometer are shifted in time with respect to the other interferometer by multiple delays much larger than the maximum GW travel time between the interferometers. In this way, we can accumulate a significant

¹The cWB algorithm requires at least 600 s of continuous data to perform its analysis.

duration of estimated background that we use to estimate the false-alarm rate (FAR) for each algorithm.

We set a FAR threshold of 1 in 100 yr for identifying a detection candidate, which roughly corresponds to a 3 sigma detection statement for the duration of our observation. If an event in this search were to have a FAR less than this threshold, a refined analysis (i.e., more time shifts) would be performed to assign the appropriate significance in the detection statement for this event.

A. Coherent WaveBurst

Coherent WaveBurst has been used in multiple searches for transient GWs [14,25]. It calculates a maximum-likelihood-ratio statistic for power excesses identified in the time-frequency domain. A primary selection cut is applied to the network correlation coefficient c_c , which measures the degree of correlation between the detectors. Events with $c_c < 0.7$ are discarded from the analysis. Events are ranked according to their coherent network signal-to-noise ratio (SNR) η_c , which is related to the matched-filter SNR, favoring GW signals correlated in both detectors and suppressing uncorrelated glitches. A detailed explanation of the algorithm and the definition of these statistics are given in Ref. [7].

The cWB analysis is divided in two frequency bands, where the splitting frequency is 1024 Hz. For the low-frequency band, the data are downsampled to reduce the computational cost of the analysis.

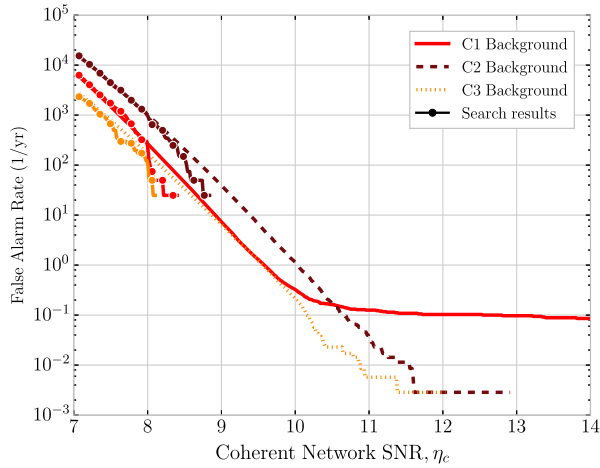
Low-frequency cWB events are divided into three search classes according to their morphology, as described in Ref. [7]. The C1 class is based on cuts which primarily select so-called “blip” glitches and nonstationary power-spectrum lines. The former are non-Gaussian noise transients of unknown origin consisting of a few cycles around 100 Hz. The C3 class is based on cuts that select events of which the frequency increases with time, i.e., those similar in morphology to the merger of compact objects. The C2 class is composed of all the remaining events.

The FAR of each identified event is estimated using the time-slide background distribution of similar class. Since there are three independent classes, we apply a trials factor of 3 to estimate the final significance. The high-frequency analysis consists of only a single class.

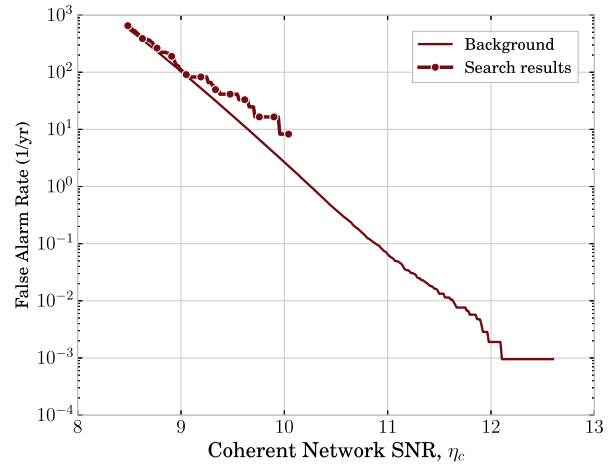
About 1000 yr of coincident background data were accumulated for the cWB analysis. Figures 1(a) and 1(b) report the cumulative FAR as a function of η_c for the low-frequency and high-frequency analyses, respectively, including the three different classes for the low-frequency case.

B. Omicron-LIB

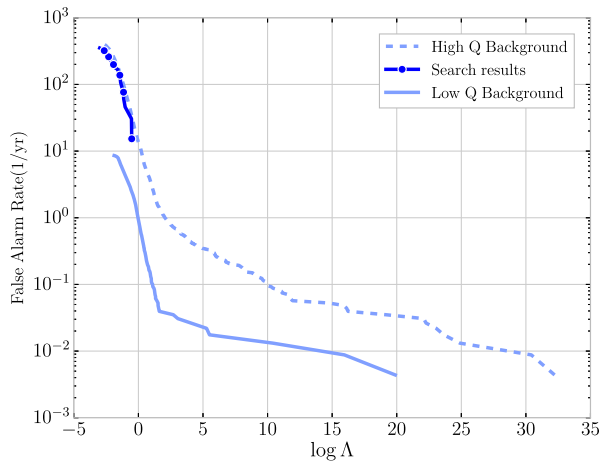
Omicron-LIB is a hierarchical search algorithm that first analyzes the data streams of individual detectors, which we refer to as an incoherent analysis. It then follows up stretches of data that are potentially correlated across the detector network, which we refer to as a coherent analysis.



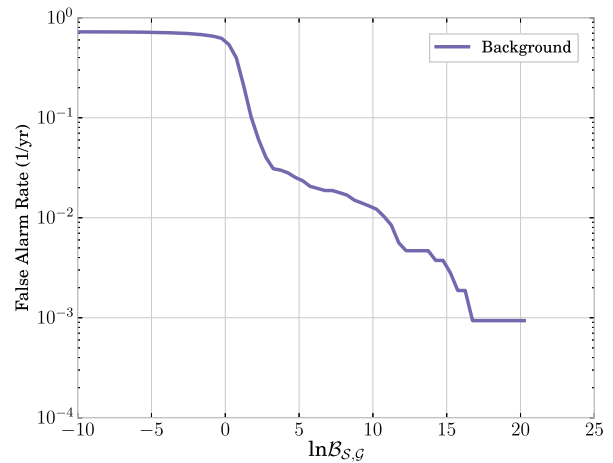
(a) **cWB** 32-1024 Hz search classes: C1 (red), C2 (brown), C3 (yellow).



(b) **cWB** 1024-4096 Hz search class.



(c) **oLIB** 48-1024 Hz low- Q (dashed) and high- Q (solid) search classes.



(d) **BayesWave** followup to **cWB** 32-1024 Hz search class.

FIG. 1. Search results and backgrounds as a function of the detection statistic for the different searches. The FAR refers to the rate (after trials factors are applied) at which events more significant than the corresponding detection statistic occur. If the results of a search deviate from its background, we use the background FAR to characterize the significance of the deviation being caused by noise alone. Apart from GW150914 (which is not reported in these figures), the search results are consistent with the expectations of accidental noise coincidences.

The incoherent analysis (“Omicron”) [33] flags stretches of coincident excess power. The coherent followup (“LIB”) [18] models gravitational-wave signals and noise transients with a single sine-Gaussian, and it produces two different Bayes factors. Each of these Bayes factors is expressed as the natural logarithm of the evidence ratio of two hypotheses: a GW signal vs Gaussian noise (Bayes factor coherent Signal vs Gaussian Noise (BSN)) and a coherent GW signal vs incoherent noise transients (Bayes factor Coherent signal vs Incoherent glitch (BCI)). The joint likelihood ratio Λ of these two Bayes factors is used as a ranking statistic to assign a significance to each event. See Ref. [18] for further technical details on the implementation of these steps.

For this analysis, oLIB events are divided into two classes, based on the inferred parameters of the best-fit

sine-Gaussian. The exact parameter ranges of these search classes are chosen in order to group noise transients of similar morphology together. Particularly noisy regions of the parameter space are excluded from the analysis entirely (e.g., events with median quality factor $Q > 108$). Both classes contain only events of which the median frequency f_0 , as estimated by LIB, lies within the range of 48–1024 Hz. The first, analogous to cWB’s C1 class, is a “low- Q ” class that contains only events of which the median quality factor Q lies within the range 0.1–2. The second, analogous to the union of cWB’s C2 and C3 classes, is a “high- Q ” class that contains only events of which the median Q lies within the range 2–108. In both classes, event candidates were also required to have positive Bayes factors, i.e., $BSN > 0$ and $BCI > 0$,

meaning the evidence for the signal model was greater than the evidences for the noise models. A trials factor of 2 accounts for these independent search classes.

The oLIB background analysis is performed using 456 yr of background data. We select single-detector events with $\text{SNR} > 5.0$. This is lower than the threshold of 6.5 adopted in Ref. [7], and it is chosen to allow us to make a significance estimation of low-SNR events. For this reason, we cannot directly compare the two sets of results reported in Ref. [7] and in this study using the likelihood ratios Λ , but we have to consider the reported FAR. The results are presented in Fig. 1(c).

C. BayesWave followup

BayesWave tests if the data in multiple detectors are best explained by coincident glitches or a signal, and it is used as a followup to events produced by cWB. It has been shown that BW is able to increase the detection confidence for GW signals of complex morphology [16].

The BW algorithm uses a variable number of sine-Gaussian wavelets to reconstruct the data independently for the signal and glitch models, then computes the natural logarithm of the Bayes factor between these two models, $\ln \mathcal{B}_{sg}$. The number of wavelets used is determined by using a reversible jump Markov chain Monte Carlo, with more complex signals requiring more wavelets [17]. The Bayes factor scales as $\ln \mathcal{B}_{sg} \sim N \ln \text{SNR}$, where N is number of wavelets used. This means the detection statistic depends on waveform complexity in addition to the SNR. Full details of the algorithm can be found in Ref. [30].

In this search, BW followed up events produced by cWB in any of the three low-frequency search classes with a coherent network SNR of $\eta_c \geq 9.9$ and correlation coefficient of $c_c > 0.7$. There are no additional cuts performed on the data, and all of these events (C1 + C2 + C3) are analyzed as a single class. The cumulative FAR as a function of $\ln \mathcal{B}_{sg}$ is shown in Fig. 1(d).

IV. SENSITIVITY

The detection efficiency of the search is measured by adding simulated signals into the detectors' data and evaluating whether or not they pass the selection cuts explained in Sec. III for the different search algorithms. This search deals with a wide range of GW sources that are usually not well modeled. However, they can be represented with a variety of morphologies that were tested here, spanning a wide range of amplitudes and duration, and with characteristic frequencies within the sensitive bandwidth of the detectors. We identify two different waveform sets: a set of generic bursts and a set of simulated astrophysical signals coming from the coalescence and merging of binary black holes (BBH). All of the results in this section refer to a FAR detection threshold of 1 in 100 yr.

TABLE I. The h_{rss} values, in units of $10^{-22} \text{ Hz}^{-1/2}$, at which 50% detection efficiency is achieved at a FAR of 1 in 100 yr for each of the algorithms, as a function of the injected signal morphologies. "N/A" denotes that 50% detection efficiency was not achieved. "-" denotes the waveform was not analyzed by oLIB and BW because its characteristic frequency is higher than 1024 Hz.

Morphology	cWB	oLIB	BW
<i>Gaussian pulses</i>			
$\tau = 0.1 \text{ ms}$	34	N/A	N/A
$\tau = 2.5 \text{ ms}$	33	7.4	N/A
<i>Sine-Gaussian wavelets</i>			
$f_0 = 70 \text{ Hz}, Q = 100$	24	N/A	N/A
$f_0 = 153 \text{ Hz}, Q = 8.9$	1.6	1.7	5.4
$f_0 = 235 \text{ Hz}, Q = 100$	14	1.9	N/A
$f_0 = 554 \text{ Hz}, Q = 8.9$	2.6	2.7	3.6
$f_0 = 849 \text{ Hz}, Q = 3$	27	3.3	5.4
$f_0 = 1615 \text{ Hz}, Q = 100$	5.5	-	-
$f_0 = 2000 \text{ Hz}, Q = 3$	8.7	-	-
$f_0 = 2477 \text{ Hz}, Q = 8.9$	11	-	-
$f_0 = 3067 \text{ Hz}, Q = 3$	15	-	-
<i>White-noise bursts</i>			
$f_{\text{low}} = 100 \text{ Hz}, \Delta f = 100 \text{ Hz}, \tau = 0.1 \text{ s}$	2.0	N/A	3.0
$f_{\text{low}} = 250 \text{ Hz}, \Delta f = 100 \text{ Hz}, \tau = 0.1 \text{ s}$	2.2	N/A	9.2

A. Generic bursts

This family includes the waveform types described in Ref. [24], all with elliptical polarization: *Gaussian pulses* (GA), parametrized by their duration parameter τ ; *sine-Gaussian wavelets* (SG), sinusoids within a Gaussian envelope, characterized by the frequency of the sinusoid f_0 and a quality factor Q ; *white-noise bursts*, white noise bounded in frequency over a bandwidth Δf and with a Gaussian envelope, described by the lower frequency f_{low} , Δf , and the duration τ . Table I lists the waveforms that have been considered for this work.

The amplitudes of the test signals are chosen to cover a wide range of values and are expressed in terms of the root-mean-square strain amplitude at Earth (before accounting for the detection response patterns), denoted h_{rss} [14].

Table I shows the h_{rss} value at which 50% of the injections are detected for each signal morphology and algorithm. There are some morphology-dependent features that affect each of the different algorithms at the FAR threshold of 1 in 100 yr. These features largely disappear, and the different algorithms' results converge at detection thresholds of higher FAR. For example, the detection efficiencies are worse for cWB for low- Q morphologies and high- Q morphologies because these injections are classified as C1 events. As shown in Fig. 1(a), the C1 background extends to higher significances than in the other bins, meaning these high- Q and low- Q events must

have large values of η_c to meet the FAR threshold of 1 in 100 yr. The oLIB detection efficiencies, while non-negligible across all morphologies, never quite reach 50% for some non-sine-Gaussian morphologies because the template mismatch residuals grow linearly with h_{rss} . Finally, the detection efficiencies of BW suffers for high- Q events since its prior range only extends to $Q = 40$. However, almost every morphology can be detected efficiently by at least one of the algorithms.

Another way to interpret the search sensitivities is to map them into the minimum amount of energy that needs to be emitted through GWs for at least half of the sources to be detected within a given search volume. Assuming a fixed amount of energy is radiated isotropically away from the source in GWs of a fixed frequency f_0 , this distance r_0 can be converted into a value of h_{rss} via the relationship [14]

$$E_{\text{GW}} = \frac{\pi^2 c^3}{G} r_0^2 f_0^2 h_{\text{rss}}^2. \quad (1)$$

Here, we use the h_{rss} from Table I, the central frequency of each morphology, and a fixed fiducial radius to calculate this energy via Eq. (1). Figure 2 shows this energy as a function of characteristic frequency assuming a galactic source at a distance of 10 kpc.² When taking into account the results of all three algorithms, this emission energy is not strongly dependent on the type of waveform (with exceptions on an algorithm-by-algorithm basis, as described above). Figure 2 can easily be converted to other distances by applying the scaling relation suggested by Eq. (1). Previous studies [14] have published similar emission-energy-vs-frequency plots at a detection threshold of 1 in 8 yr. We note that the current results, when evaluated at this higher-FAR threshold, are roughly an order of magnitude more sensitive than these previous results, due mainly to the improvement in detector sensitivities.

B. Binary black holes mergers

We also consider a set of astrophysical waveforms using models of merging of binary black hole systems. Specifically, we choose the SEOBNRv2 model as implemented in the LAL software library [34,35]. The waveforms are generated with an initial frequency of 15 Hz. The simulated binary systems are isotropically located in the sky and isotropically oriented. The total redshifted mass of

²Eq. (1) holds under the assumption that the source emits gravitational waves monochromatically. For most of our injections, this conditional is well-approximated by the central frequency of the injection. However, because Gaussians have a central frequency of 0 Hz, they are only detectable due to their broadband nature. Thus, Eq. (1) does not give physically meaningful results for Gaussian injections, and we neglect them in Fig. 2.

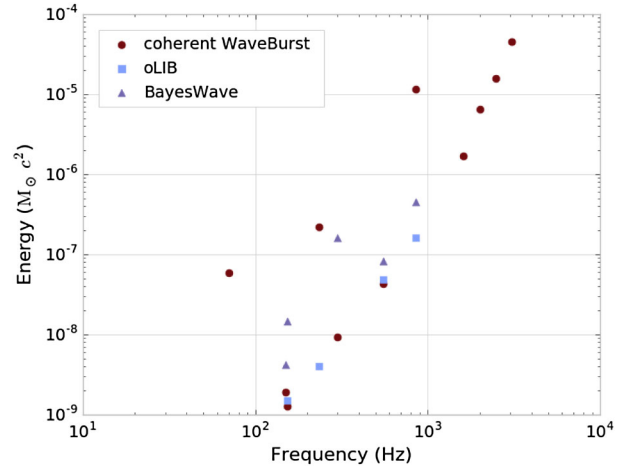


FIG. 2. GW emission energy, in solar masses, at 50% detection efficiency for standard-candle sources emitting at 10 kpc for the non-GA waveforms listed in Table I. These results can be scaled to any reference distance r_0 using $E_{\text{GW}} \propto r_0^2$.

the system in the detector frame³ is distributed uniformly between 10 and 150 M_\odot , a range that encompasses the total masses of both GW150914 and GW151226 [22]. The black hole spins are aligned with the binary angular momentum, and the magnitude of the dimensionless spin vector, $\mathbf{a}_{1,2}$, is uniformly distributed between 0 and 0.99. We neglect any cosmological corrections, such as normalizing our spatial distribution to be constant in comoving volume. We generate three different injection sets, each one with a mass ratio $q = m_2/m_1$ chosen from the set $\{0.25, 0.5, 1.0\}$ (where m_1 is by definition the more massive object).

In Fig. 3, we compare the sensitive luminosity radius [36] as a function of the total redshifted mass in the detector frame. While systems inside this distance may be missed and systems outside of it may be detected depending on their sky position and orientation, this sensitive radius provides a “rule-of-thumb” determination on whether or not this burst search will detect a system’s GW transients. We can see that for systems like GW150914 ($\sim 70M_\odot$ [37]) and GW151226 ($\sim 20M_\odot$ [22]), the search ranges at the FAR of 1/100 yr are approximately 500–700 and 100–200 Mpc, respectively. These ranges demonstrates why this search detects GW150914 (~ 400 Mpc [37]) but not GW151226 (~ 400 Mpc [22]). Even though the two sources are at a similar luminosity distance, this burst search is less efficient at detecting low-mass BBH systems. This behavior is true for two reasons: lower-mass systems emit less energy into GWs than higher-mass systems, and this energy is distributed over a longer duration of time. These two features make it more difficult for nontemplated

³Given the luminosity distance of the system, one can assume a cosmology and calculate its redshift z . The system’s total mass in the source frame can then be obtained by dividing the total redshifted mass in the detector frame by $(1+z)$.

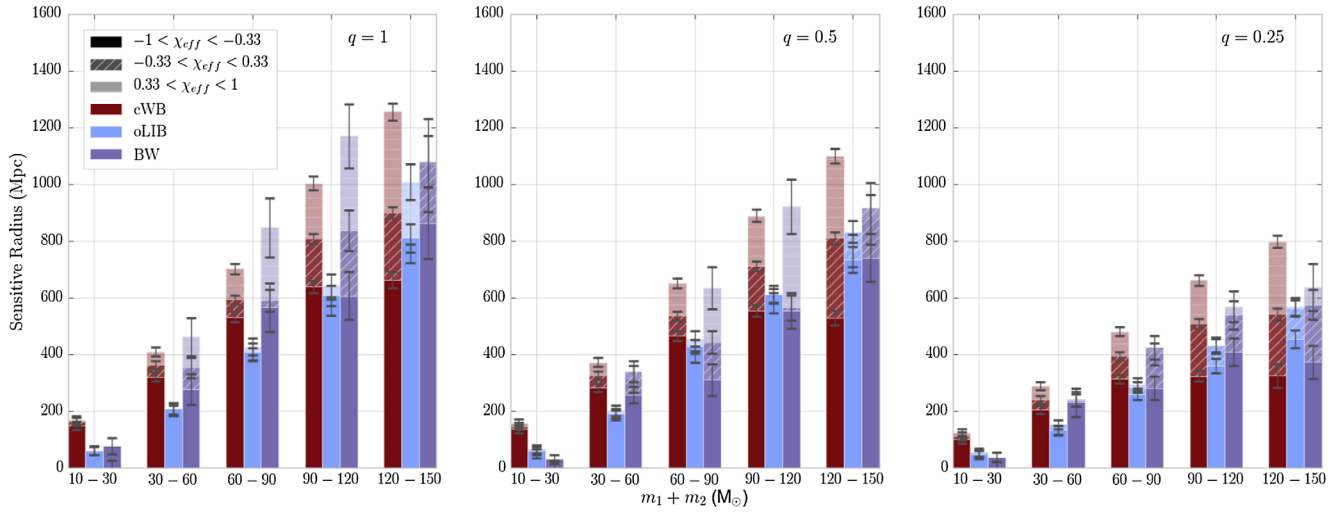


FIG. 3. A comparison of the sensitive luminosity radii [7] in Mpc, as a function of the total redshifted masses in the detector frame, among the three algorithms. The radii are binned according to mass ratio q (from left to right $q = 1, 0.5, 0.25$) and effective spin χ_{eff} , defined in Ref. [7]. The three ranges of spin refer to aligned ($0.33 < \chi_{\text{eff}} < 1$), nonspinning ($-0.33 < \chi_{\text{eff}} < 0.33$), and antialigned ($-1 < \chi_{\text{eff}} < -0.33$).

algorithms to extract the GW signal from the detector noise as compared to searches based on templates.

V. RESULTS

The most significant event and only detection established in this search is GW150914 [3], which is independently confirmed by all three algorithms. Specifically, it is found by cWB in the C3 class of the low-frequency analysis with an estimated FAR of less than 1 in 350 yr, by oLIB in the “high- Q ” class with an estimated FAR of less than 1 in 230 yr, and by BayesWave with an estimated FAR of less than 1 in 1000 yr.⁴ These results are less precise but consistent with Ref. [3].

All other events generated by the analyses are consistent with the accidental noise coincidence rates. To be specific, there are no other events found above the SNR thresholds in either the low- Q class of oLIB or the entire BayesWave analysis bin. The rate of other events in the oLIB high- Q bin are consistent with the accidental noise coincidence rates within 1 sigma. The event in the cWB analysis with the second-lowest FAR belongs to the high frequency search, with a false-alarm probability of about 0.2.

These results set constraints on the population of transient GW sources within the volume of the Universe that the detectors were sensitive to during O1. Again, all of the results in this section refer to a FAR detection threshold of 1 in 100 yr.

We estimate the limits on the rate density of generic non-BBH-like GW-burst sources in Fig. 4 by removing the known BBH detections GW150914 and GW151226 from

our analysis. We emphasize that, although we remove the resolved BBH detections from our analysis, these upper limits may be contaminated by any unresolved BBH signals still present in the data. We use the sine-Gaussian injection set as a representative morphology and present our cWB rate-density estimates as a function of their characteristic frequencies. The bands represent the 90% confidence intervals on rate density [14], calculated using the Feldman-Cousins formalism for zero background events [38]. The frequency-dependent variation among the

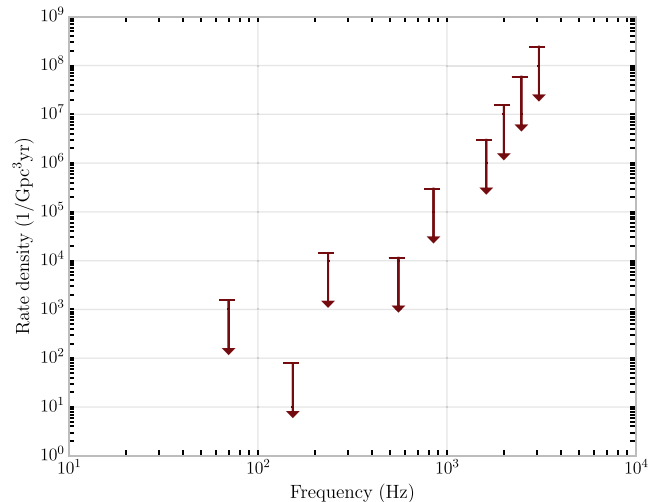


FIG. 4. The 90% confidence intervals of rate density given by the cWB pipeline for the sine-Gaussian waveforms listed in Table I. This plot assumes zero detections, zero background, and that $1 M_{\odot} c^2$ of energy is emitted in gravitational waves. These results can be scaled to any emission energy E_{GW} using $\text{rate density} \propto E_{\text{GW}}^{-3/2}$. The arrow markers signify that the confidence intervals extend to zero.

⁴Because GW150914 was louder than any of the background events in this search, we can only provide the relatively unprecise upper limits on FAR listed above.

upper limits is due to the sine-Gaussians falling into different cWB search classes as a result of their specific value of Q . For a given value of Q , the results follow a smoother frequency dependence. These results are not directly comparable with those from previous runs [14] because of the different FAR detection thresholds. However, we note that at the previously used FAR detection threshold of 1 in 8 yr our search lowers these upper limits by about an order of magnitude across all frequencies. The sensitivity improvements of the detectors and pipelines allow us to make these stricter rate statements even though we analyzed less live time compared to Ref. [14] (less than 50 days compared to 1.7 yr). Figure 4 assumes $1 M_{\odot} c^2$ of gravitational-wave energy has been emitted from the source, but this can be scaled to any emission energy E_{GW} by using Eq. (1). Note that the rate density scales as $\propto E_{\text{GW}}^{-\frac{3}{2}}$.

VI. DISCUSSION

This paper reports the results for the search for short-duration GW in the first Advanced LIGO observing run, with minimal assumptions on the signal waveform, direction, or arrival time. The two LIGO detectors, Livingston and Hanford, were operating from mid-September 2015 to mid-January 2016, with a greater sensitivity to GWs than any previous LIGO-Virgo run. This search has been performed considering two end-to-end algorithms and a followup algorithm.

The only detection established in this search is the GW150914 event, a binary system consisting of two black holes merging to form a single one [3]. The other known black hole detection [20] falls below the sensitivity of this search, and all other events in the search result are consistent with accidental noise coincidences between the detectors.

We report the minimum GW emission energy needed to detect at least half of the transient events emitted within some fiducial distance. These energies depend primarily on the signal frequency and are approximately constant over the different models of GW emission morphology. We also estimate rate-density limits on non-BBH transient sources as a function of their frequency and their gravitational-wave emission energy.

The interferometric detectors LIGO and Virgo are currently being upgraded for the next scientific run. LIGO should improve its sensitivity over the next few years, Virgo should soon come online, and the implementation of KAGRA and LIGO India is also in progress. All of these

improvements will allow this type of unmodeled search to achieve a better sensitivity in the future [6].

ACKNOWLEDGMENTS

The authors gratefully acknowledge the support of the United States National Science Foundation (NSF) for the construction and operation of the LIGO Laboratory and Advanced LIGO as well as the Science and Technology Facilities Council (STFC) of the United Kingdom, the Max-Planck-Society (MPS), and the State of Niedersachsen/Germany for support of the construction of Advanced LIGO and construction and operation of the GEO600 detector. Additional support for Advanced LIGO was provided by the Australian Research Council. The authors gratefully acknowledge the Italian Istituto Nazionale di Fisica Nucleare (INFN), the French Centre National de la Recherche Scientifique (CNRS), and the Foundation for Fundamental Research on Matter supported by the Netherlands Organisation for Scientific Research, for the construction and operation of the Virgo detector and the creation and support of the European Gravitational Observatory (EGO) consortium. The authors also gratefully acknowledge research support from these agencies as well as by the Council of Scientific and Industrial Research of India, Department of Science and Technology, India, Science & Engineering Research Board, India; Ministry of Human Resource Development, India; the Spanish Ministerio de Economía y Competitividad, the Conselleria d'Economia i Competitivitat and Conselleria d'Educació, Cultura i Universitats of the Govern de les Illes Balears; the National Science Centre of Poland; the European Commission; the Royal Society; the Scottish Funding Council; the Scottish Universities Physics Alliance; the Hungarian Scientific Research Fund; the Lyon Institute of Origins; the National Research Foundation of Korea; Industry Canada and the Province of Ontario through the Ministry of Economic Development and Innovation; the Natural Science and Engineering Research Council Canada; Canadian Institute for Advanced Research; the Brazilian Ministry of Science, Technology, and Innovation, Fundação de Amparo à Pesquisa do Estado de São Paulo (FAPESP); Russian Foundation for Basic Research; the Leverhulme Trust; the Research Corporation; Ministry of Science and Technology, Taiwan; and the Kavli Foundation. The authors gratefully acknowledge the support of the NSF, STFC, MPS, INFN, CNRS, and the State of Niedersachsen/Germany for the provision of computational resources.

- [1] J. Aasi *et al.*, Characterization of the LIGO detectors during their sixth science run, *Classical Quantum Gravity* **32**, 115012 (2015).
- [2] F. Acernese *et al.*, Advanced Virgo: A second-generation interferometric gravitational wave detector, *Classical Quantum Gravity* **32**, 024001 (2015).
- [3] B. Abbott *et al.*, Observation of Gravitational Waves from a Binary Black Hole Merger, *Phys. Rev. Lett.* **116**, 061102 (2016).
- [4] H. Lück, C. Affeldt, J. Degallaix, A. Freise, H. Grote, M. Hewitson, S. Hild, J. Leong, M. Prijatelj, K. A. Strain, B. Willke, H. Wittel, and K. Danzmann, The upgrade of GEO600, *J. Phys. Conf. Ser.* **228**, 012012 (2010).
- [5] Y. Aso, Y. Michimura, K. Somiya, M. Ando, O. Miyakawa, T. Sekiguchi, D. Tatsumi, and H. Yamamoto, Interferometer design of the KAGRA gravitational wave detector, *Phys. Rev. D* **88**, 043007 (2013).
- [6] J. Aasi *et al.*, Prospects for observing and localizing gravitational-wave transients with Advanced LIGO and Advanced Virgo, *Living Rev. Relativ.* **19**, 1 (2016).
- [7] B. Abbott *et al.*, Observing gravitational-wave transient GW150914 with minimal assumptions, *Phys. Rev. D* **93**, 122004 (2016).
- [8] J. Aasi *et al.*, Search for gravitational radiation from intermediate mass black hole binaries in data from the second LIGO-Virgo joint science run, *Phys. Rev. D* **89**, 122003 (2014).
- [9] S. Mohapatra, L. Cadonati, S. Caudill, J. Clark, C. Hanna, S. Klimenko, C. Pankow, R. Vaulin, G. Vedovato, and S. Vitale, Sensitivity comparison of searches for binary black hole coalescences with ground-based gravitational-wave detectors, *Phys. Rev. D* **90**, 022001 (2014).
- [10] C. L. Fryer and K. C. B. New, Gravitational waves from gravitational collapse, *Living Rev. Relativ.* **14**, 1 (2011).
- [11] T. Damour and A. Vilenkin, Gravitational radiation from cosmic (super)strings: Bursts, stochastic background, and observational windows, *Phys. Rev. D* **71**, 063510 (2005).
- [12] B. P. Abbott *et al.*, A first targeted search for gravitational-wave bursts from core-collapse supernovae in data of first-generation laser interferometer detectors, *Phys. Rev. D* **94**, 102001 (2016).
- [13] K. Hurley and A. Rau, The Status and Future of the Third Inter-planetary Network, In: *Gamma Ray Bursts*, in *AIP Conference Proceedings*, No. 1133 (American Institute of Physics, Melville, NY, 2009), pp. 55–57, <http://resolver.caltech.edu/CaltechAUTHORS:20160505-162423876>.
- [14] J. Abadie *et al.*, All-sky search for gravitational-wave bursts in the second joint LIGO-Virgo run, *Phys. Rev. D* **85**, 122007 (2012).
- [15] J. Aasi *et al.*, Characterization of the LIGO detectors during their sixth science run, *Classical Quantum Gravity* **32**, 115012 (2015).
- [16] J. B. Kanner, T. B. Littenberg, N. Cornish, M. Millhouse, E. Xhakaj, F. Salemi, M. Drago, G. Vedovato, and S. Klimenko, Leveraging waveform complexity for confident detection of gravitational waves, *Phys. Rev. D* **93**, 022002 (2016).
- [17] T. B. Littenberg, J. B. Kanner, N. J. Cornish, and M. Millhouse, Enabling high confidence detections of gravitational-wave bursts, *Phys. Rev. D* **94**, 044050 (2016).
- [18] R. Lynch, S. Vitale, R. Essick, E. Katsavounidis, and F. Robinet, An information-theoretic approach to the gravitational-wave burst detection problem, [arXiv:1511.05955](https://arxiv.org/abs/1511.05955).
- [19] S. Klimenko, G. Vedovato, M. Drago, F. Salemi, V. Tiwari, G. A. Prodi, C. Lazzaro, S. Tiwari, F. Da Silva, and G. Mitselmakher, Method for detection and reconstruction of gravitational wave transients with networks of advanced detectors, *Phys. Rev. D* **93**, 042004 (2016).
- [20] B. Abbott *et al.*, GW151226: Observation of Gravitational Waves from a 22-Solar-Mass Binary Black Hole Coalescence, *Phys. Rev. Lett.* **116**, 241103 (2016).
- [21] B. Abbott *et al.*, GW150914: First results from the search for binary black hole coalescence with Advanced LIGO, *Phys. Rev. D* **93**, 122003 (2016).
- [22] B. Abbott *et al.*, Binary Black Hole Mergers in the first Advanced LIGO Observing Run, *Phys. Rev. X* **6**, 041015 (2016).
- [23] B. P. Abbott *et al.*, An all-sky search for long-duration gravitational wave transients with LIGO, *Phys. Rev. D* **93**, 042005 (2016).
- [24] J. Abadie *et al.*, All-sky search for gravitational-wave bursts in the second joint LIGO-Virgo run, *Phys. Rev. D* **85**, 122007 (2012).
- [25] J. Abadie *et al.*, All-sky search for gravitational-wave bursts in the first joint LIGO-GEO-Virgo run, *Phys. Rev. D* **81**, 102001 (2010).
- [26] B. Abbott *et al.*, Characterization of transient noise in Advanced LIGO relevant to gravitational wave signal GW150914, *Class. Quant. Grav.* **33**, 134001 (2016).
- [27] B. Abbott *et al.*, Calibration of the Advanced LIGO detectors for the discovery of the binary black-hole merger GW150914, [arXiv:1602.03845](https://arxiv.org/abs/1602.03845).
- [28] C. Callihane and J. Kissel (private communication).
- [29] S. Klimenko, I. Yakushin, A. Mercer, and Guenakh Mitselmakher, Coherent method for detection of gravitational wave bursts, *Classical Quantum Gravity* **25**, 114029 (2008).
- [30] N. J. Cornish and T. B. Littenberg, BayesWave: Bayesian Inference for Gravitational Wave Bursts and Instrument Glitches, *Classical Quantum Gravity* **32**, 135012 (2015).
- [31] T. B. Littenberg and N. J. Cornish, Bayesian inference for spectral estimation of gravitational wave detector noise, *Phys. Rev. D* **91**, 084034 (2015).
- [32] B. Abbott *et al.*, Localization and broadband follow-up of the gravitational-wave transient GW150914, *Astrophys. J. Lett.* **826**, L13 (2016).
- [33] F. Robinet, Omicron: An algorithm to detect and characterize transient noise in gravitational-wave detectors, <https://tds.ego-gw.it/ql/?c=10651>, 2015.
- [34] A. Taracchini, A. Buonanno, Y. Pan, T. Hinderer, M. Boyle, D. A. Hemberger, L. E. Kidder, G. Lovelace, A. H. Mroué, H. P. Pfeiffer, M. A. Scheel, B. Szilágyi, N. W. Taylor, and A. Zenginoglu, Effective-one-body model for black-hole binaries with generic mass ratios and spins, *Phys. Rev. D* **89**, 061502 (2014).
- [35] P. Kumar, K. Barkett, S. Bhagwat, N. Afshari, D. A. Brown, G. Lovelace, M. A. Scheel, and B. Szilágyi, Accuracy and precision of gravitational-wave models of inspiraling neutron star-black hole binaries with spin: Comparison with

- matter-free numerical relativity in the low-frequency regime, *Phys. Rev. D* **92**, 102001 (2015).
- [36] J. Abadie *et al.* (LIGO Scientific and Virgo Collaborations), Search for gravitational waves from intermediate mass binary black holes, *Phys. Rev. D* **85**, 102004 (2012).
- [37] B. Abbott *et al.*, Properties of the Binary Black Hole Merger GW150914, *Phys. Rev. Lett.* **116**, 241102 (2016).
- [38] G. J. Feldman and R. D. Cousins, A unified approach to the classical statistical analysis of small signals, *Phys. Rev. D* **57**, 3873 (1998).
-
- B. P. Abbott,¹ R. Abbott,¹ T. D. Abbott,² M. R. Abernathy,³ F. Acernese,^{4,5} K. Ackley,⁶ C. Adams,⁷ T. Adams,⁸ P. Addesso,⁹ R. X. Adhikari,¹ V. B. Adya,¹⁰ C. Affeldt,¹⁰ M. Agathos,¹¹ K. Agatsuma,¹¹ N. Aggarwal,¹² O. D. Aguiar,¹³ L. Aiello,^{14,15} A. Ain,¹⁶ B. Allen,^{10,17,18} A. Allocca,^{19,20} P. A. Altin,²¹ A. Ananyeva,¹ S. B. Anderson,¹ W. G. Anderson,¹⁷ S. Appert,¹ K. Arai,¹ M. C. Araya,¹ J. S. Areeda,²² N. Arnaud,²³ K. G. Arun,²⁴ S. Ascenzi,^{25,15} G. Ashton,¹⁰ M. Ast,²⁶ S. M. Aston,⁷ P. Astone,²⁷ P. Aufmuth,¹⁸ C. Aulbert,¹⁰ A. Avila-Alvarez,²² S. Babak,²⁸ P. Bacon,²⁹ M. K. M. Bader,¹¹ P. T. Baker,³⁰ F. Baldaccini,^{31,32} G. Ballardín,³³ S. W. Ballmer,³⁴ J. C. Barayoga,¹ S. E. Barclay,³⁵ B. C. Barish,¹ D. Barker,³⁶ F. Barone,^{4,5} B. Barr,³⁵ L. Barsotti,¹² M. Barsuglia,²⁹ D. Barta,³⁷ J. Bartlett,³⁶ I. Bartos,³⁸ R. Bassiri,³⁹ A. Basti,^{19,20} J. C. Batch,³⁶ C. Baune,¹⁰ V. Bavigada,³³ M. Bazzan,^{40,41} C. Beer,¹⁰ M. Bejger,⁴² I. Belahcene,²³ M. Belgin,⁴³ A. S. Bell,³⁵ B. K. Berger,¹ G. Bergmann,¹⁰ C. P. L. Berry,⁴⁴ D. Bersanetti,^{45,46} A. Bertolini,¹¹ J. Betzwieser,⁷ S. Bhagwat,³⁴ R. Bhandare,⁴⁷ I. A. Bilenko,⁴⁸ G. Billingsley,¹ C. R. Billman,⁶ J. Birch,⁷ R. Birney,⁴⁹ O. Birnholtz,¹⁰ S. Biscans,^{12,1} A. Bisht,¹⁸ M. Bitossi,³³ C. Biwer,³⁴ M. A. Bizouard,²³ J. K. Blackburn,¹ J. Blackman,⁵⁰ C. D. Blair,⁵¹ D. G. Blair,⁵¹ R. M. Blair,³⁶ S. Bloemen,⁵² O. Bock,¹⁰ M. Boer,⁵³ G. Bogaert,⁵³ A. Bohe,²⁸ F. Bondu,⁵⁴ R. Bonnand,⁸ B. A. Boom,¹¹ R. Bork,¹ V. Boschi,^{19,20} S. Bose,^{55,16} Y. Bouffanais,²⁹ A. Bozzi,³³ C. Bradaschia,²⁰ P. R. Brady,¹⁷ V. B. Braginsky,^{48,†} M. Branchesi,^{56,57} J. E. Brau,⁵⁸ T. Briant,⁵⁹ A. Brillet,⁵³ M. Brinkmann,¹⁰ V. Brisson,²³ P. Brockill,¹⁷ J. E. Broida,⁶⁰ A. F. Brooks,¹ D. A. Brown,³⁴ D. D. Brown,⁴⁴ N. M. Brown,¹² S. Brunett,¹ C. C. Buchanan,² A. Buikema,¹² T. Bulik,⁶¹ H. J. Bulten,^{62,11} A. Buonanno,^{28,63} D. Buskulic,⁸ C. Buy,²⁹ R. L. Byer,³⁹ M. Cabero,¹⁰ L. Cadonati,⁴³ G. Cagnoli,^{64,65} C. Cahillane,¹ J. Calderón Bustillo,⁴³ T. A. Callister,¹ E. Calloni,^{66,5} J. B. Camp,⁶⁷ M. Canepa,^{45,46} K. C. Cannon,⁶⁸ H. Cao,⁶⁹ J. Cao,⁷⁰ C. D. Capano,¹⁰ E. Capocasa,²⁹ F. Carbognani,³³ S. Caride,⁷¹ J. Casanueva Diaz,²³ C. Casentini,^{25,15} S. Caudill,¹⁷ M. Cavaglià,⁷² F. Cavalier,²³ R. Cavalieri,³³ G. Cella,²⁰ C. B. Cepeda,¹ L. Cerboni Baiardi,^{56,57} G. Cerretani,^{19,20} E. Cesarini,^{25,15} S. J. Chamberlin,⁷³ M. Chan,³⁵ S. Chao,⁷⁴ P. Charlton,⁷⁵ E. Chassande-Mottin,²⁹ B. D. Cheeseboro,³⁰ H. Y. Chen,⁷⁶ Y. Chen,⁵⁰ H.-P. Cheng,⁶ A. Chincarini,⁴⁶ A. Chiummo,³³ T. Chmiel,⁷⁷ H. S. Cho,⁷⁸ M. Cho,⁶³ J. H. Chow,²¹ N. Christensen,⁶⁰ Q. Chu,⁵¹ A. J. K. Chua,⁷⁹ S. Chua,⁵⁹ S. Chung,⁵¹ G. Ciani,⁶ F. Clara,³⁶ J. A. Clark,⁴³ F. Cleva,⁵³ C. Cocchieri,⁷² E. Coccia,^{14,15} P.-F. Cohadon,⁵⁹ A. Colla,^{80,27} C. G. Collette,⁸¹ L. Cominsky,⁸² M. Constancio Jr.,¹³ L. Conti,⁴¹ S. J. Cooper,⁴⁴ T. R. Corbitt,² N. Cornish,⁸³ A. Corsi,⁷¹ S. Cortese,³³ C. A. Costa,¹³ M. W. Coughlin,⁶⁰ S. B. Coughlin,⁸⁴ J.-P. Coulon,⁵³ S. T. Countryman,³⁸ P. Couvares,¹ P. B. Covas,⁸⁵ E. E. Cowan,⁴³ D. M. Coward,⁵¹ M. J. Cowart,⁷ D. C. Coyne,¹ R. Coyne,⁷¹ J. D. E. Creighton,¹⁷ T. D. Creighton,⁸⁶ J. Cripe,² S. G. Crowder,⁸⁷ T. J. Cullen,²² A. Cumming,³⁵ L. Cunningham,³⁵ E. Cuoco,³³ T. Dal Canton,⁶⁷ S. L. Danilishin,³⁵ S. D'Antonio,¹⁵ K. Danzmann,^{18,10} A. Dasgupta,⁸⁸ C. F. Da Silva Costa,⁶ V. Dattilo,³³ I. Dave,⁴⁷ M. Davier,²³ G. S. Davies,³⁵ D. Davis,³⁴ E. J. Daw,⁸⁹ B. Day,⁴³ R. Day,³³ S. De,³⁴ D. DeBra,³⁹ G. Debreczeni,³⁷ J. Degallaix,⁶⁴ M. De Laurentis,^{66,5} S. Deléglise,⁵⁹ W. Del Pozzo,⁴⁴ T. Denker,¹⁰ T. Dent,¹⁰ V. Dergachev,²⁸ R. De Rosa,^{66,5} R. T. DeRosa,⁷ R. DeSalvo,⁹⁰ J. Devenson,⁴⁹ R. C. Devine,³⁰ S. Dhurandhar,¹⁶ M. C. Díaz,⁸⁶ L. Di Fiore,⁵ M. Di Giovanni,^{91,92} T. Di Girolamo,^{66,5} A. Di Lieto,^{19,20} S. Di Pace,^{80,27} I. Di Palma,^{28,80,27} A. Di Virgilio,²⁰ Z. Doctor,⁷⁶ V. Dolique,⁶⁴ F. Donovan,¹² K. L. Dooley,⁷² S. Doravari,¹⁰ I. Dorrington,⁹³ R. Douglas,³⁵ M. Dovale Álvarez,⁴⁴ T. P. Downes,¹⁷ M. Drago,¹⁰ R. W. P. Drever,¹ J. C. Driggers,³⁶ Z. Du,⁷⁰ M. Ducrot,⁸ S. E. Dwyer,³⁶ T. B. Edo,⁸⁹ M. C. Edwards,⁶⁰ A. Effler,⁷ H.-B. Eggenstein,¹⁰ P. Ehrens,¹ J. Eichholz,¹ S. S. Eikenberry,⁶ R. A. Eisenstein,¹² R. C. Essick,¹² Z. Etienne,³⁰ T. Etzel,¹ M. Evans,¹² T. M. Evans,⁷ R. Everett,⁷³ M. Factourovich,³⁸ V. Fafone,^{25,15,14} H. Fair,³⁴ S. Fairhurst,⁹³ X. Fan,⁷⁰ S. Farinon,⁴⁶ B. Farr,⁷⁶ W. M. Farr,⁴⁴ E. J. Fauchon-Jones,⁹³ M. Favata,⁹⁴ M. Fays,⁹³ H. Fehrmann,¹⁰ M. M. Fejer,³⁹ A. Fernández Galiana,¹² I. Ferrante,^{19,20} E. C. Ferreira,¹³ F. Ferrini,³³ F. Fidecaro,^{19,20} I. Fiori,³³ D. Fiorucci,²⁹ R. P. Fisher,³⁴ R. Flaminio,^{64,95} M. Fletcher,³⁵ H. Fong,⁹⁶ S. S. Forsyth,⁴³ J.-D. Fournier,⁵³ S. Frasca,^{80,27} F. Frasconi,²⁰ Z. Frei,⁹⁷ A. Freise,⁴⁴ R. Frey,⁵⁸ V. Frey,²³ E. M. Fries,¹ P. Fritschel,¹² V. V. Frolov,⁷ P. Fulda,^{6,67} M. Fyffe,⁷ H. Gabbard,¹⁰ B. U. Gadre,¹⁶ S. M. Gaebel,⁴⁴ J. R. Gair,⁹⁸ L. Gammaitoni,³¹ S. G. Gaonkar,¹⁶ F. Garufi,^{66,5} G. Gaur,⁹⁹ V. Gayathri,¹⁰⁰ N. Gehrels,⁶⁷ G. Gemme,⁴⁶ E. Genin,³³ A. Gennai,²⁰ J. George,⁴⁷ L. Gergely,¹⁰¹ V. Germain,⁸ S. Ghonge,¹⁰² Abhirup Ghosh,¹⁰² Archisman Ghosh,^{11,102} S. Ghosh,^{52,11} J. A. Giaime,^{2,7}

K. D. Giardina,⁷ A. Giazotto,²⁰ K. Gill,¹⁰³ A. Glaefke,³⁵ E. Goetz,¹⁰ R. Goetz,⁶ L. Gondan,⁹⁷ G. González,² J. M. Gonzalez Castro,^{19,20} A. Gopakumar,¹⁰⁴ M. L. Gorodetsky,⁴⁸ S. E. Gossan,¹ M. Gosselin,³³ R. Gouaty,⁸ A. Grado,^{105,5} C. Graef,³⁵ M. Granata,⁶⁴ A. Grant,³⁵ S. Gras,¹² C. Gray,³⁶ G. Greco,^{56,57} A. C. Green,⁴⁴ P. Groot,⁵² H. Grote,¹⁰ S. Grunewald,²⁸ G. M. Guidi,^{56,57} X. Guo,⁷⁰ A. Gupta,¹⁶ M. K. Gupta,⁸⁸ K. E. Gushwa,¹ E. K. Gustafson,¹ R. Gustafson,¹⁰⁶ J. J. Hacker,²² B. R. Hall,⁵⁵ E. D. Hall,¹ G. Hammond,³⁵ M. Haney,¹⁰⁴ M. M. Hanke,¹⁰ J. Hanks,³⁶ C. Hanna,⁷³ J. Hanson,⁷ T. Hardwick,² J. Harms,^{56,57} G. M. Harry,³ I. W. Harry,²⁸ M. J. Hart,³⁵ M. T. Hartman,⁶ C.-J. Haster,^{44,96} K. Haughian,³⁵ J. Healy,¹⁰⁷ A. Heidmann,⁵⁹ M. C. Heintze,⁷ H. Heitmann,⁵³ P. Hello,²³ G. Hemming,³³ M. Hendry,³⁵ I. S. Heng,³⁵ J. Hennig,³⁵ J. Henry,¹⁰⁷ A. W. Heptonstall,¹ M. Heurs,^{10,18} S. Hild,³⁵ D. Hoak,³³ D. Hofman,⁶⁴ K. Holt,⁷ D. E. Holz,⁷⁶ P. Hopkins,⁹³ J. Hough,³⁵ E. A. Houston,³⁵ E. J. Howell,⁵¹ Y. M. Hu,¹⁰ E. A. Huerta,¹⁰⁸ D. Huet,²³ B. Hughey,¹⁰³ S. Husa,⁸⁵ S. H. Huttner,³⁵ T. Huynh-Dinh,⁷ N. Indik,¹⁰ D. R. Ingram,³⁶ R. Inta,⁷¹ H. N. Isa,³⁵ J.-M. Isac,⁵⁹ M. Isi,¹ T. Isogai,¹² B. R. Iyer,¹⁰² K. Izumi,³⁶ T. Jacqmin,⁵⁹ K. Jani,⁴³ P. Jaranowski,¹⁰⁹ S. Jawahar,¹¹⁰ F. Jiménez-Forteza,⁸⁵ W. W. Johnson,² D. I. Jones,¹¹¹ R. Jones,³⁵ R. J. G. Jonker,¹¹ L. Ju,⁵¹ J. Junker,¹⁰ C. V. Kalaghatgi,⁹³ S. Kandhasamy,⁷² G. Kang,⁷⁸ J. B. Kanner,¹ S. Karki,⁵⁸ K. S. Karvinen,¹⁰ M. Kasprzack,² E. Katsavounidis,¹² W. Katzman,⁷ S. Kaufer,¹⁸ T. Kaur,⁵¹ K. Kawabe,³⁶ F. Kéfélian,⁵³ D. Keitel,⁸⁵ D. B. Kelley,³⁴ R. Kennedy,⁸⁹ J. S. Key,¹¹² F. Y. Khalili,⁴⁸ I. Khan,¹⁴ S. Khan,⁹³ Z. Khan,⁸⁸ E. A. Khazanov,¹¹³ N. Kijbunchoo,³⁶ Chunglee Kim,¹¹⁴ J. C. Kim,¹¹⁵ Whansun Kim,¹¹⁶ W. Kim,⁶⁹ Y.-M. Kim,^{117,114} S. J. Kimbrell,⁴³ E. J. King,⁶⁹ P. J. King,³⁶ R. Kirchhoff,¹⁰ J. S. Kissel,³⁶ B. Klein,⁸⁴ L. Kleybolte,²⁶ S. Klimenko,⁶ P. Koch,¹⁰ S. M. Koehlenbeck,¹⁰ S. Koley,¹¹ V. Kondrashov,¹ A. Kontos,¹² M. Korobko,²⁶ W. Z. Korth,¹ I. Kowalska,⁶¹ D. B. Kozak,¹ C. Krämer,¹⁰ V. Kringel,¹⁰ B. Krishnan,¹⁰ A. Królak,^{118,119} G. Kuehn,¹⁰ P. Kumar,⁹⁶ R. Kumar,⁸⁸ L. Kuo,⁷⁴ A. Kutynia,¹¹⁸ B. D. Lackey,^{28,34} M. Landry,³⁶ R. N. Lang,¹⁷ J. Lange,¹⁰⁷ B. Lantz,³⁹ R. K. Lanza,¹² A. Lartaux-Vollard,²³ P. D. Lasky,¹²⁰ M. Laxen,⁷ A. Lazzarini,¹ C. Lazzaro,⁴¹ P. Leaci,^{80,27} S. Leavey,³⁵ E. O. Lebigot,²⁹ C. H. Lee,¹¹⁷ H. K. Lee,¹²¹ H. M. Lee,¹¹⁴ K. Lee,³⁵ J. Lehmann,¹⁰ A. Lenon,³⁰ M. Leonardi,^{91,92} J. R. Leong,¹⁰ N. Leroy,²³ N. Letendre,⁸ Y. Levin,¹²⁰ T. G. F. Li,¹²² A. Libson,¹² T. B. Littenberg,¹²³ J. Liu,⁵¹ N. A. Lockerbie,¹¹⁰ A. L. Lombardi,⁴³ L. T. London,⁹³ J. E. Lord,³⁴ M. Lorenzini,^{14,15} V. Lorette,¹²⁴ M. Lormand,⁷ G. Losurdo,²⁰ J. D. Lough,^{10,18} G. Lovelace,²² H. Lüch,^{18,10} A. P. Lundgren,¹⁰ R. Lynch,¹² Y. Ma,⁵⁰ S. Macfoy,⁴⁹ B. Machenschalk,¹⁰ M. MacInnis,¹² D. M. Macleod,² F. Magaña-Sandoval,³⁴ E. Majorana,²⁷ I. Maksimovic,¹²⁴ V. Malvezzi,^{25,15} N. Man,⁵³ V. Mandic,¹²⁵ V. Mangano,³⁵ G. L. Mansell,²¹ M. Manske,¹⁷ M. Mantovani,³³ F. Marchesoni,^{126,32} F. Marion,⁸ S. Márka,³⁸ Z. Márka,³⁸ A. S. Markosyan,³⁹ E. Maros,¹ F. Martelli,^{56,57} L. Martellini,⁵³ I. W. Martin,³⁵ D. V. Martynov,¹² K. Mason,¹² A. Masserot,⁸ T. J. Massinger,¹ M. Masso-Reid,³⁵ S. Mastrogiovanni,^{80,27} F. Matichard,^{12,1} L. Matone,³⁸ N. Mavalvala,¹² N. Mazumder,⁵⁵ R. McCarthy,³⁶ D. E. McClelland,²¹ S. McCormick,⁷ C. McGrath,¹⁷ S. C. McGuire,¹²⁷ G. McIntyre,¹ J. McIver,¹ D. J. McManus,²¹ T. McRae,²¹ S. T. McWilliams,³⁰ D. Meacher,^{53,73} G. D. Meadors,^{28,10} J. Meidam,¹¹ A. Melatos,¹²⁸ G. Mendell,³⁶ D. Mendoza-Gandara,¹⁰ R. A. Mercer,¹⁷ E. L. Merilh,³⁶ M. Merzougui,⁵³ S. Meshkov,¹ C. Messenger,³⁵ C. Messick,⁷³ R. Metzдорff,⁵⁹ P. M. Meyers,¹²⁵ F. Mezzani,^{27,80} H. Miao,⁴⁴ C. Michel,⁶⁴ H. Middleton,⁴⁴ E. E. Mikhailov,¹²⁹ L. Milano,^{66,5} A. L. Miller,^{6,80,27} A. Miller,⁸⁴ B. B. Miller,⁸⁴ J. Miller,¹² M. Millhouse,⁸³ Y. Minenkov,¹⁵ J. Ming,²⁸ S. Mirshekari,¹³⁰ C. Mishra,¹⁰² S. Mitra,¹⁶ V. P. Mitrofanov,⁴⁸ G. Mitselmakher,⁶ R. Mittleman,¹² A. Moggi,²⁰ M. Mohan,³³ S. R. P. Mohapatra,¹² M. Montani,^{56,57} B. C. Moore,⁹⁴ C. J. Moore,⁷⁹ D. Moraru,³⁶ G. Moreno,³⁶ S. R. Morriss,⁸⁶ B. Mours,⁸ C. M. Mow-Lowry,⁴⁴ G. Mueller,⁶ A. W. Muir,⁹³ Arunava Mukherjee,¹⁰² D. Mukherjee,¹⁷ S. Mukherjee,⁸⁶ N. Mukund,¹⁶ A. Mullavey,⁷ J. Munch,⁶⁹ E. A. M. Muniz,²² P. G. Murray,³⁵ A. Mytidis,⁶ K. Napier,⁴³ I. Nardecchia,^{25,15} L. Naticchioni,^{80,27} G. Nelemans,^{52,11} T. J. N. Nelson,⁷ M. Neri,^{45,46} M. Nery,¹⁰ A. Neunzert,¹⁰⁶ J. M. Newport,³ G. Newton,³⁵ T. T. Nguyen,²¹ S. Nissanke,^{52,11} A. Nitz,¹⁰ A. Noack,¹⁰ F. Nocera,³³ D. Nolting,⁷ M. E. N. Normandin,⁸⁶ L. K. Nuttall,³⁴ J. Oberling,³⁶ E. Ochsner,¹⁷ E. Oelker,¹² G. H. Ogin,¹³¹ J. J. Oh,¹¹⁶ S. H. Oh,¹¹⁶ F. Ohme,^{93,10} M. Oliver,⁸⁵ P. Oppermann,¹⁰ Richard J. Oram,⁷ B. O'Reilly,⁷ R. O'Shaughnessy,¹⁰⁷ D. J. Ottaway,⁶⁹ H. Overmier,⁷ B. J. Owen,⁷¹ A. E. Pace,⁷³ J. Page,¹²³ A. Pai,¹⁰⁰ S. A. Pai,⁴⁷ J. R. Palamos,⁵⁸ O. Palashov,¹¹³ C. Palomba,²⁷ A. Pal-Singh,²⁶ H. Pan,⁷⁴ C. Pankow,⁸⁴ F. Pannarale,⁹³ B. C. Pant,⁴⁷ F. Paoletti,^{33,20} A. Paoli,³³ M. A. Papa,^{28,17,10} H. R. Paris,³⁹ W. Parker,⁷ D. Pascucci,³⁵ A. Pasqualetti,³³ R. Passaquieti,^{19,20} D. Passuello,²⁰ B. Patricelli,^{19,20} B. L. Pearlstone,³⁵ M. Pedraza,¹ R. Pedurand,^{64,132} L. Pekowsky,³⁴ A. Pele,⁷ S. Penn,¹³³ C. J. Perez,³⁶ A. Perreca,¹ L. M. Perri,⁸⁴ H. P. Pfeiffer,⁹⁶ M. Phelps,³⁵ O. J. Piccinni,^{80,27} M. Pichot,⁵³ F. Piergiovanni,^{56,57} V. Pierro,⁹ G. Pillant,³³ L. Pinard,⁶⁴ I. M. Pinto,⁹ M. Pitkin,³⁵ M. Poe,¹⁷ R. Poggiani,^{19,20} P. Popolizio,³³ A. Post,¹⁰ J. Powell,³⁵ J. Prasad,¹⁶ J. W. W. Pratt,¹⁰³ V. Predoi,⁹³ T. Prestegard,^{125,17} M. Prijatelj,^{10,33} M. Principe,⁹ S. Privitera,²⁸ G. A. Prodi,^{91,92} L. G. Prokhorov,⁴⁸ O. Puncken,¹⁰ M. Punturo,³² P. Puppó,²⁷ M. Pürerer,²⁸ H. Qi,¹⁷ J. Qin,⁵¹ S. Qiu,¹²⁰ V. Quetschke,⁸⁶ E. A. Quintero,¹ R. Quitzow-James,⁵⁸ F. J. Raab,³⁶ D. S. Rabeling,²¹

H. Radkins,³⁶ P. Raffai,⁹⁷ S. Raja,⁴⁷ C. Rajan,⁴⁷ M. Rakhmanov,⁸⁶ P. Rapagnani,^{80,27} V. Raymond,²⁸ M. Razzano,^{19,20} V. Re,²⁵ J. Read,²² T. Regimbau,⁵³ L. Rei,⁴⁶ S. Reid,⁴⁹ D. H. Reitze,^{1,6} H. Rew,¹²⁹ S. D. Reyes,³⁴ E. Rhoades,¹⁰³ F. Ricci,^{80,27} K. Riles,¹⁰⁶ M. Rizzo,¹⁰⁷ N. A. Robertson,^{1,35} R. Robie,³⁵ F. Robinet,²³ A. Rocchi,¹⁵ L. Rolland,⁸ J. G. Rollins,¹ V. J. Roma,⁵⁸ R. Romano,^{4,5} J. H. Romie,⁷ D. Rosińska,^{134,42} S. Rowan,³⁵ A. Rüdiger,¹⁰ P. Ruggi,³³ K. Ryan,³⁶ S. Sachdev,¹ T. Sadecki,³⁶ L. Sadeghian,¹⁷ M. Sakellariadou,¹³⁵ L. Salconi,³³ M. Saleem,¹⁰⁰ F. Salemi,¹⁰ A. Samajdar,¹³⁶ L. Sammut,¹²⁰ L. M. Sampson,⁸⁴ E. J. Sanchez,¹ V. Sandberg,³⁶ J. R. Sanders,³⁴ B. Sassolas,⁶⁴ B. S. Sathyaprakash,^{73,93} P. R. Saulson,³⁴ O. Sauter,¹⁰⁶ R. L. Savage,³⁶ A. Sawadsky,¹⁸ P. Schale,⁵⁸ J. Scheuer,⁸⁴ E. Schmidt,¹⁰³ J. Schmidt,¹⁰ P. Schmidt,^{1,50} R. Schnabel,²⁶ R. M. S. Schofield,⁵⁸ A. Schönbeck,²⁶ E. Schreiber,¹⁰ D. Schuette,^{10,18} B. F. Schutz,^{93,28} S. G. Schwalbe,¹⁰³ J. Scott,³⁵ S. M. Scott,²¹ D. Sellers,⁷ A. S. Sengupta,¹³⁷ D. Sentenac,³³ V. Sequino,^{25,15} A. Sergeev,¹¹³ Y. Setyawati,^{52,11} D. A. Shaddock,²¹ T. J. Shaffer,³⁶ M. S. Shariar,⁸⁴ B. Shapiro,³⁹ P. Shawhan,⁶³ A. Sheperd,¹⁷ D. H. Shoemaker,¹² D. M. Shoemaker,⁴³ K. Siellez,⁴³ X. Siemens,¹⁷ M. Sieniawska,⁴² D. Sigg,³⁶ A. D. Silva,¹³ A. Singer,¹ L. P. Singer,⁶⁷ A. Singh,^{28,10,18} R. Singh,² A. Singhal,¹⁴ A. M. Sintes,⁸⁵ B. J. J. Slagmolen,²¹ B. Smith,⁷ J. R. Smith,²² R. J. E. Smith,¹ E. J. Son,¹¹⁶ B. Sorazu,³⁵ F. Sorrentino,⁴⁶ T. Souradeep,¹⁶ A. P. Spencer,³⁵ A. K. Srivastava,⁸⁸ A. Staley,³⁸ M. Steinke,¹⁰ J. Steinlechner,³⁵ S. Steinlechner,^{26,35} D. Steinmeyer,^{10,18} B. C. Stephens,¹⁷ S. P. Stevenson,⁴⁴ R. Stone,⁸⁶ K. A. Strain,³⁵ N. Straniero,⁶⁴ G. Stratta,^{56,57} S. E. Strigin,⁴⁸ R. Sturani,¹³⁰ A. L. Stuver,⁷ T. Z. Summerscales,¹³⁸ L. Sun,¹²⁸ S. Sunil,⁸⁸ P. J. Sutton,⁹³ B. L. Swinkels,³³ M. J. Szczepańczyk,¹⁰³ M. Tacca,²⁹ D. Talukder,⁵⁸ D. B. Tanner,⁶ M. Tápai,¹⁰¹ A. Taracchini,²⁸ R. Taylor,¹ T. Theeg,¹⁰ E. G. Thomas,⁴⁴ M. Thomas,⁷ P. Thomas,³⁶ K. A. Thorne,⁷ E. Thrane,¹²⁰ T. Tippens,⁴³ S. Tiwari,^{14,92} V. Tiwari,⁹³ K. V. Tokmakov,¹¹⁰ K. Toland,³⁵ C. Tomlinson,⁸⁹ M. Tonelli,^{19,20} Z. Tornasi,³⁵ C. I. Torrie,¹ D. Töyrä,⁴⁴ F. Travasso,^{31,32} G. Traylor,⁷ D. Trifirò,⁷² J. Trinastic,⁶ M. C. Tringali,^{91,92} L. Trozzo,^{139,20} M. Tse,¹² R. Tso,¹ M. Turconi,⁵³ D. Tuyenbayev,⁸⁶ D. Ugolini,¹⁴⁰ C. S. Unnikrishnan,¹⁰⁴ A. L. Urban,¹ S. A. Usman,⁹³ H. Vahlbruch,¹⁸ G. Vajente,¹ G. Valdes,⁸⁶ N. van Bakel,¹¹ M. van Beuzekom,¹¹ J. F. J. van den Brand,^{62,11} C. Van Den Broeck,¹¹ D. C. Vander-Hyde,³⁴ L. van der Schaaf,¹¹ J. V. van Heijningen,¹¹ A. A. van Veggel,³⁵ M. Vardaro,^{40,41} V. Varma,⁵⁰ S. Vass,¹ M. Vasúth,³⁷ A. Vecchio,⁴⁴ G. Vedovato,⁴¹ J. Veitch,⁴⁴ P. J. Veitch,⁶⁹ K. Venkateswara,¹⁴¹ G. Venugopalan,¹ D. Verkindt,⁸ F. Vetrano,^{56,57} A. Viceré,^{56,57} A. D. Viets,¹⁷ S. Vinciguerra,⁴⁴ D. J. Vine,⁴⁹ J.-Y. Vinet,⁵³ S. Vitale,¹² T. Vo,³⁴ H. Vocca,^{31,32} C. Vorvick,³⁶ D. V. Voss,⁶ W. D. Voudsen,⁴⁴ S. P. Vyatchanin,⁴⁸ A. R. Wade,¹ L. E. Wade,⁷⁷ M. Wade,⁷⁷ M. Walker,² L. Wallace,¹ S. Walsh,^{28,10} G. Wang,^{14,57} H. Wang,⁴⁴ M. Wang,⁴⁴ Y. Wang,⁵¹ R. L. Ward,²¹ J. Warner,³⁶ M. Was,⁸ J. Watchi,⁸¹ B. Weaver,³⁶ L.-W. Wei,⁵³ M. Weinert,¹⁰ A. J. Weinstein,¹ R. Weiss,¹² L. Wen,⁵¹ P. Weßels,¹⁰ T. Westphal,¹⁰ K. Wette,¹⁰ J. T. Whelan,¹⁰⁷ B. F. Whiting,⁶ C. Whittle,¹²⁰ D. Williams,³⁵ R. D. Williams,¹ A. R. Williamson,⁹³ J. L. Willis,¹⁴² B. Willke,^{18,10} M. H. Wimmer,^{10,18} W. Winkler,¹⁰ C. C. Wipf,¹ H. Wittel,^{10,18} G. Woan,³⁵ J. Woehler,¹⁰ J. Worden,³⁶ J. L. Wright,³⁵ D. S. Wu,¹⁰ G. Wu,⁷ W. Yam,¹² H. Yamamoto,¹ C. C. Yancey,⁶³ M. J. Yap,²¹ Hang Yu,¹² Haocun Yu,¹² M. Yvert,⁸ A. Zadrożny,¹¹⁸ L. Zangrando,⁴¹ M. Zanolin,¹⁰³ J.-P. Zendri,⁴¹ M. Zevin,⁸⁴ L. Zhang,¹ M. Zhang,¹²⁹ T. Zhang,³⁵ Y. Zhang,¹⁰⁷ C. Zhao,⁵¹ M. Zhou,⁸⁴ Z. Zhou,⁸⁴ S. J. Zhu,^{28,10} X. J. Zhu,⁵¹ M. E. Zucker,^{1,12} and J. Zweigig¹

(LIGO Scientific Collaboration and Virgo Collaboration)

¹LIGO, California Institute of Technology, Pasadena, California 91125, USA

²Louisiana State University, Baton Rouge, Louisiana 70803, USA

³American University, Washington, D.C. 20016, USA

⁴Università di Salerno, Fisciano, I-84084 Salerno, Italy

⁵INFN, Sezione di Napoli, Complesso Universitario di Monte S. Angelo, I-80126 Napoli, Italy

⁶University of Florida, Gainesville, Florida 32611, USA

⁷LIGO Livingston Observatory, Livingston, Louisiana 70754, USA

⁸Laboratoire d'Annecy-le-Vieux de Physique des Particules (LAPP), Université Savoie Mont Blanc, CNRS/IN2P3, F-74941 Annecy-le-Vieux, France

⁹University of Sannio at Benevento, I-82100 Benevento, Italy
and INFN, Sezione di Napoli, I-80100 Napoli, Italy

¹⁰Albert-Einstein-Institut, Max-Planck-Institut für Gravitationsphysik, D-30167 Hannover, Germany

¹¹Nikhef, Science Park, 1098 XG Amsterdam, Netherlands

¹²LIGO, Massachusetts Institute of Technology, Cambridge, Massachusetts 02139, USA

¹³Instituto Nacional de Pesquisas Espaciais, 12227-010 São José dos Campos, São Paulo, Brazil

¹⁴INFN, Gran Sasso Science Institute, I-67100 L'Aquila, Italy

¹⁵INFN, Sezione di Roma Tor Vergata, I-00133 Roma, Italy

- ¹⁶*Inter-University Centre for Astronomy and Astrophysics, Pune 411007, India*
- ¹⁷*University of Wisconsin-Milwaukee, Milwaukee, Wisconsin 53201, USA*
- ¹⁸*Leibniz Universität Hannover, D-30167 Hannover, Germany*
- ¹⁹*Università di Pisa, I-56127 Pisa, Italy*
- ²⁰*INFN, Sezione di Pisa, I-56127 Pisa, Italy*
- ²¹*Australian National University, Canberra, Australian Capital Territory 0200, Australia*
- ²²*California State University Fullerton, Fullerton, California 92831, USA*
- ²³*LAL, Univ. Paris-Sud, CNRS/IN2P3, Université Paris-Saclay, F-91898 Orsay, France*
- ²⁴*Chennai Mathematical Institute, Chennai 603103, India*
- ²⁵*Università di Roma Tor Vergata, I-00133 Roma, Italy*
- ²⁶*Universität Hamburg, D-22761 Hamburg, Germany*
- ²⁷*INFN, Sezione di Roma, I-00185 Roma, Italy*
- ²⁸*Albert-Einstein-Institut, Max-Planck-Institut für Gravitationsphysik, D-14476 Potsdam-Golm, Germany*
- ²⁹*APC, AstroParticule et Cosmologie, Université Paris Diderot, CNRS/IN2P3, CEA/Irfu, Observatoire de Paris, Sorbonne Paris Cité, F-75205 Paris Cedex 13, France*
- ³⁰*West Virginia University, Morgantown, West Virginia 26506, USA*
- ³¹*Università di Perugia, I-06123 Perugia, Italy*
- ³²*INFN, Sezione di Perugia, I-06123 Perugia, Italy*
- ³³*European Gravitational Observatory (EGO), I-56021 Cascina, Pisa, Italy*
- ³⁴*Syracuse University, Syracuse, New York 13244, USA*
- ³⁵*SUPA, University of Glasgow, Glasgow G12 8QQ, United Kingdom*
- ³⁶*LIGO Hanford Observatory, Richland, Washington 99352, USA*
- ³⁷*Wigner RCP, RMKI, H-1121 Budapest, Konkoly Thege Miklós út 29-33, Hungary*
- ³⁸*Columbia University, New York, New York 10027, USA*
- ³⁹*Stanford University, Stanford, California 94305, USA*
- ⁴⁰*Università di Padova, Dipartimento di Fisica e Astronomia, I-35131 Padova, Italy*
- ⁴¹*INFN, Sezione di Padova, I-35131 Padova, Italy*
- ⁴²*Nicolaus Copernicus Astronomical Center, Polish Academy of Sciences, 00-716 Warsaw, Poland*
- ⁴³*Center for Relativistic Astrophysics and School of Physics, Georgia Institute of Technology, Atlanta, Georgia 30332, USA*
- ⁴⁴*University of Birmingham, Birmingham B15 2TT, United Kingdom*
- ⁴⁵*Università degli Studi di Genova, I-16146 Genova, Italy*
- ⁴⁶*INFN, Sezione di Genova, I-16146 Genova, Italy*
- ⁴⁷*RRCAT, Indore, Madhya Pradesh 452013, India*
- ⁴⁸*Faculty of Physics, Lomonosov Moscow State University, Moscow 119991, Russia*
- ⁴⁹*SUPA, University of the West of Scotland, Paisley PA1 2BE, United Kingdom*
- ⁵⁰*Caltech CaRT, Pasadena, California 91125, USA*
- ⁵¹*University of Western Australia, Crawley, Western Australia 6009, Australia*
- ⁵²*Department of Astrophysics/IMAPP, Radboud University Nijmegen, P.O. Box 9010, 6500 GL Nijmegen, Netherlands*
- ⁵³*Artemis, Université Côte d'Azur, CNRS, Observatoire Côte d'Azur, CS 34229, F-06304 Nice Cedex 4, France*
- ⁵⁴*Institut de Physique de Rennes, CNRS, Université de Rennes 1, F-35042 Rennes, France*
- ⁵⁵*Washington State University, Pullman, Washington 99164, USA*
- ⁵⁶*Università degli Studi di Urbino 'Carlo Bo', I-61029 Urbino, Italy*
- ⁵⁷*INFN, Sezione di Firenze, I-50019 Sesto Fiorentino, Firenze, Italy*
- ⁵⁸*University of Oregon, Eugene, Oregon 97403, USA*
- ⁵⁹*Laboratoire Kastler Brossel, UPMC-Sorbonne Universités, CNRS, ENS-PSL Research University, Collège de France, F-75005 Paris, France*
- ⁶⁰*Carleton College, Northfield, Minnesota 55057, USA*
- ⁶¹*Astronomical Observatory Warsaw University, 00-478 Warsaw, Poland*
- ⁶²*VU University Amsterdam, 1081 HV Amsterdam, Netherlands*
- ⁶³*University of Maryland, College Park, Maryland 20742, USA*
- ⁶⁴*Laboratoire des Matériaux Avancés (LMA), CNRS/IN2P3, F-69622 Villeurbanne, France*
- ⁶⁵*Université Claude Bernard Lyon 1, F-69622 Villeurbanne, France*
- ⁶⁶*Università di Napoli 'Federico II', Complesso Universitario di Monte S. Angelo, I-80126 Napoli, Italy*
- ⁶⁷*NASA/Goddard Space Flight Center, Greenbelt, Maryland 20771, USA*
- ⁶⁸*RESCEU, University of Tokyo, Tokyo, 113-0033, Japan*
- ⁶⁹*University of Adelaide, Adelaide, South Australia 5005, Australia*
- ⁷⁰*Tsinghua University, Beijing 100084, China*

- ⁷¹Texas Tech University, Lubbock, Texas 79409, USA
- ⁷²The University of Mississippi, University, Mississippi 38677, USA
- ⁷³The Pennsylvania State University, University Park, Pennsylvania 16802, USA
- ⁷⁴National Tsing Hua University, Hsinchu City, 30013 Taiwan, Republic of China
- ⁷⁵Charles Sturt University, Wagga Wagga, New South Wales 2678, Australia
- ⁷⁶University of Chicago, Chicago, Illinois 60637, USA
- ⁷⁷Kenyon College, Gambier, Ohio 43022, USA
- ⁷⁸Korea Institute of Science and Technology Information, Daejeon 305-806, Korea
- ⁷⁹University of Cambridge, Cambridge CB2 1TN, United Kingdom
- ⁸⁰Università di Roma 'La Sapienza', I-00185 Roma, Italy
- ⁸¹University of Brussels, Brussels 1050, Belgium
- ⁸²Sonoma State University, Rohnert Park, California 94928, USA
- ⁸³Montana State University, Bozeman, Montana 59717, USA
- ⁸⁴Center for Interdisciplinary Exploration & Research in Astrophysics (CIERA), Northwestern University, Evanston, Illinois 60208, USA
- ⁸⁵Universitat de les Illes Balears, IAC3—IEEC, E-07122 Palma de Mallorca, Spain
- ⁸⁶The University of Texas Rio Grande Valley, Brownsville, Texas 78520, USA
- ⁸⁷Bellevue College, Bellevue, Washington 98007, USA
- ⁸⁸Institute for Plasma Research, Bhat, Gandhinagar 382428, India
- ⁸⁹The University of Sheffield, Sheffield S10 2TN, United Kingdom
- ⁹⁰California State University, Los Angeles, 5154 State University Dr, Los Angeles, California 90032, USA
- ⁹¹Università di Trento, Dipartimento di Fisica, I-38123 Povo, Trento, Italy
- ⁹²INFN, Trento Institute for Fundamental Physics and Applications, I-38123 Povo, Trento, Italy
- ⁹³Cardiff University, Cardiff CF24 3AA, United Kingdom
- ⁹⁴Montclair State University, Montclair, New Jersey 07043, USA
- ⁹⁵National Astronomical Observatory of Japan, 2-21-1 Osawa, Mitaka, Tokyo 181-8588, Japan
- ⁹⁶Canadian Institute for Theoretical Astrophysics, University of Toronto, Toronto, Ontario M5S 3H8, Canada
- ⁹⁷MTA Eötvös University, "Lendulet" Astrophysics Research Group, Budapest 1117, Hungary
- ⁹⁸School of Mathematics, University of Edinburgh, Edinburgh EH9 3FD, United Kingdom
- ⁹⁹University and Institute of Advanced Research, Gandhinagar, Gujarat 382007, India
- ¹⁰⁰IISER-TVM, CET Campus, Trivandrum Kerala 695016, India
- ¹⁰¹University of Szeged, Dóm tér 9, Szeged 6720, Hungary
- ¹⁰²International Centre for Theoretical Sciences, Tata Institute of Fundamental Research, Bengaluru 560089, India
- ¹⁰³Embry-Riddle Aeronautical University, Prescott, Arizona 86301, USA
- ¹⁰⁴Tata Institute of Fundamental Research, Mumbai 400005, India
- ¹⁰⁵INAF, Osservatorio Astronomico di Capodimonte, I-80131 Napoli, Italy
- ¹⁰⁶University of Michigan, Ann Arbor, Michigan 48109, USA
- ¹⁰⁷Rochester Institute of Technology, Rochester, New York 14623, USA
- ¹⁰⁸NCSA, University of Illinois at Urbana-Champaign, Urbana, Illinois 61801, USA
- ¹⁰⁹University of Białystok, 15-424 Białystok, Poland
- ¹¹⁰SUPA, University of Strathclyde, Glasgow G1 1XQ, United Kingdom
- ¹¹¹University of Southampton, Southampton SO17 1BJ, United Kingdom
- ¹¹²University of Washington Bothell, 18115 Campus Way NE, Bothell, Washington 98011, USA
- ¹¹³Institute of Applied Physics, Nizhny Novgorod 603950, Russia
- ¹¹⁴Seoul National University, Seoul 151-742, Korea
- ¹¹⁵Inje University Gimhae, 621-749 South Gyeongsang, Korea
- ¹¹⁶National Institute for Mathematical Sciences, Daejeon 305-390, Korea
- ¹¹⁷Pusan National University, Busan 609-735, Korea
- ¹¹⁸NCBJ, 05-400 Świerk-Otwock, Poland
- ¹¹⁹Institute of Mathematics, Polish Academy of Sciences, 00656 Warsaw, Poland
- ¹²⁰Monash University, Victoria 3800, Australia
- ¹²¹Hanyang University, Seoul 133-791, Korea
- ¹²²The Chinese University of Hong Kong, Shatin, NT, Hong Kong SAR, China
- ¹²³University of Alabama in Huntsville, Huntsville, Alabama 35899, USA
- ¹²⁴ESPCI, CNRS, F-75005 Paris, France
- ¹²⁵University of Minnesota, Minneapolis, Minnesota 55455, USA
- ¹²⁶Università di Camerino, Dipartimento di Fisica, I-62032 Camerino, Italy
- ¹²⁷Southern University and A&M College, Baton Rouge, Louisiana 70813, USA

- ¹²⁸*The University of Melbourne, Parkville, Victoria 3010, Australia*
¹²⁹*College of William and Mary, Williamsburg, Virginia 23187, USA*
¹³⁰*Instituto de Física Teórica, University Estadual Paulista/ICTP South American Institute for
Fundamental Research, São Paulo, São Paulo 01140-070, Brazil*
¹³¹*Whitman College, 345 Boyer Avenue, Walla Walla, Washington 99362 USA*
¹³²*Université de Lyon, F-69361 Lyon, France*
¹³³*Hobart and William Smith Colleges, Geneva, New York 14456, USA*
¹³⁴*Janusz Gil Institute of Astronomy, University of Zielona Góra, 65-265 Zielona Góra, Poland*
¹³⁵*King's College London, University of London, London WC2R 2LS, United Kingdom*
¹³⁶*IISER-Kolkata, Mohanpur, West Bengal 741252, India*
¹³⁷*Indian Institute of Technology, Gandhinagar Ahmedabad Gujarat 382424, India*
¹³⁸*Andrews University, Berrien Springs, Michigan 49104, USA*
¹³⁹*Università di Siena, I-53100 Siena, Italy*
¹⁴⁰*Trinity University, San Antonio, Texas 78212, USA*
¹⁴¹*University of Washington, Seattle, Washington 98195, USA*
¹⁴²*Abilene Christian University, Abilene, Texas 79699, USA*

[†]Deceased.